

REPORT DOCUMENTATION PAGE

Form Approved
OMB NO. 0704-0188

Public Reporting burden for this collection of information is estimated to average 1 hour per response, including the time for reviewing instructions, searching existing data sources, gathering and maintaining the data needed, and completing and reviewing the collection of information. Send comment regarding this burden estimates or any other aspect of this collection of information, including suggestions for reducing this burden, to Washington Headquarters Services, Directorate for information Operations and Reports, 1215 Jefferson Davis Highway, Suite 1204, Arlington, VA 22202-4302, and to the Office of Management and Budget, Paperwork Reduction Project (0704-0188,) Washington, DC 20503.

1. AGENCY USE ONLY (Leave Blank)		2. REPORT DATE 30/03/02	3. REPORT TYPE AND DATES COVERED final report 08/01/98 07/31/01	
4. TITLE AND SUBTITLE Low power multifunctionality optoelectronic devices for mobile digital battlefield			5. FUNDING NUMBERS DAAG55-98-1-0358 34998-EL	
6. AUTHOR(S) Kang. L. Wang				
7. PERFORMING ORGANIZATION NAME(S) AND ADDRESS(ES) Kang L Wang Dept. of Electrical Engineering, University of California Los Angeles, CA, 90095-1594			8. PERFORMING ORGANIZATION REPORT NUMBER	
9. SPONSORING / MONITORING AGENCY NAME(S) AND ADDRESS(ES) U. S. Army Research Office P.O. Box 12211 Research Triangle Park, NC 27709-2211			10. SPONSORING / MONITORING AGENCY REPORT NUMBER	
11. SUPPLEMENTARY NOTES The views, opinions and/or findings contained in this report are those of the author(s) and should not be construed as an official Department of the Army position, policy or decision, unless so designated by other documentation.				
12 a. DISTRIBUTION / AVAILABILITY STATEMENT Approved for public release; distribution unlimited.			12 b. DISTRIBUTION CODE	
13. ABSTRACT (Maximum 200 words) We have grown high quality Ge quantum dots on Si selective epitaxial growth (SEG) facets as well as tilted Si substrates. We have also controlled the formation of the SEG mesas to achieve one-dimensional ridges on stripe Si patterns in attempt to form an ordered dot array. At 8K, the photoluminescence spectrum shows the contribution from Ge wetting layers and Ge quantum dots. Studies on the control of Ge dot positioning have been conducted. Several different configurations of the positioning have also been observed with the variation of the Ge thickness deposited. The intersubband absorption in self-assembled boron-doped and modulation-doped multiple Ge quantum dots was studied. An absorption peak in the midinfrared range is observed at room temperature by Fourier transform infrared spectroscopy, which is attributed to the transitions between the first two heavy-hole states of the Ge quantum dots. Si-based photodetectors operating at 1.3-1.55 μm for the purpose of fiber communication were studied. I-V measurement shows a low dark current density of $3 \times 10^{-5} \text{A/cm}^2$ at 1 V. A strong response at 1.3-1.5 μm was observed. Highest efficiency of 8% was observed at a bias of -2.5 V.				
14. SUBJECT TERMS self-regulation mechanism, controlled positioning, mid-IR absorption, photodetector			15. NUMBER OF PAGES 12	
			16. PRICE CODE	
17. SECURITY CLASSIFICATION OR REPORT UNCLASSIFIED	18. SECURITY CLASSIFICATION ON THIS PAGE UNCLASSIFIED	19. SECURITY CLASSIFICATION OF ABSTRACT UNCLASSIFIED	20. LIMITATION OF ABSTRACT UL	

NSN 7540-01-280-5500

Standard Form 298 (Rev.2-89)
Prescribed by ANSI Std. 239-18
298-102

Enclosure 1

Table of Content

Statement of the problem studied.....	1
Results from Grant DAAG55-98-1-0358.....	2
I: Ge quantum dots grown on Si, growth and characterization.....	2
II: Mid-IR absorption of Ge quantum dots.....	6
III: Photodetectors based on Ge quantum dots.....	9
List of all publications.....	11
List of all participating scientific personnel.....	12
Standard Form 298.....	13

REPORT DOCUMENTATION PAGE (SF298)
(Continuation Sheet)

Statement of the problem studied

I: The formation of coherent, strained three-dimensional Ge dots on planar Si substrates by MBE using Krastanov-Stanski mode. Attention was paid to the uniformity of the dot size. Structural properties were analyzed. Controlled positioning of the dots was achieved.

II: Intersubband absorption in direct and modulation doped Ge dots was studied.

III: Normal incidence photodetectors operate at 1.3-1.55 μm with Ge quantum dots were studied.

Results from Grant DAAG55-98-1-0358

Overview

The grant had been used to purchase equipment and to support the researches including the PhD dissertation researches of two graduate students, in an effort to accomplish Si-based nanostructures using a molecular beam epitaxy system. Publications and presentations from this grant are listed in the following part.

I: Ge quantum dots grown on Si, growth and characterization

(a) Ge quantum dots growth

We have performed systematic experimental studies of quantum dot deposition on the Si selective epitaxial growth (SEG) mesas as well as tilted Si substrates. It was found that it is possible to grow high quality uniform sized Ge quantum dots on the planar Si substrates. Fig. 1 shows the AFM image of uniform Ge quantum dots on planar Si (001). It can be seen that the Ge dots have a very good and uniform size distribution.

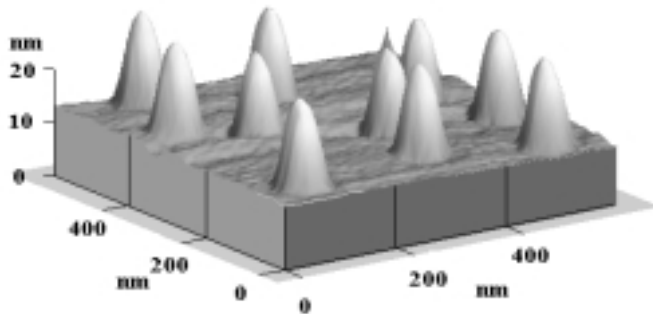


Fig. 1 An atomic force micrograph of Ge quantum dots grown on Si (100) substrate. This example demonstrates the very good control of the dot size uniformity.

One of the most critical issues in the application of quantum dots is the exact placement of dot arrays on the designated sites in addition to the control of size uniformity. Selective epitaxial growth (SEG) is an important growth technique due to its capability of fabricating devices on patterned samples without breaking the growth. During the SEG process on $\langle 110 \rangle$ -oriented patterns, $\{113\}$ facets are formed at the earlier stage of growth, leading to the shrinkage of the top surface region and finally the full reduction and formation of one-dimensional ridges. Therefore, we controlled the formation of the SEG mesas to achieve one-dimensional ridges on stripe Si patterns in an attempt to form an ordered dot array. Fig. 2 a and b present respectively two- and three-dimensional AFM images of the self-assembled Ge dots on the $\langle 110 \rangle$ -oriented Si stripe mesas, formed in the exposed Si stripe windows. Perfectly aligned and regularly spaced one-dimensional arrays of Ge dots were formed on the ridge of the Si stripe mesa. The perfect alignment of the dots along the Si stripe mesas is attributed to a self-regulation mechanism driven by the minimization of the total energy, and also assisted by the formation of the ridges. The tendency of Ge quantum dots to form on the ridge (or near the edge of a lattice step or the intersection of facet planes) is a result of stress-driven kinetics. The edges are compliant, i.e., are most easily deformed by the dots growing on the facets. The dimensions of the Ge dots are about 80 nm wide and 20 nm high, and the period of Ge dots is about 110 nm. Moreover, the aligned Ge dots showed *mono*-modal

morphology and size distribution on the ridges, which is very interesting as *bi*-(even *multi*-) modal distribution of self-assembled Ge dots is normally observed on planar Si (001) substrates. The *mono*-modal distribution is believed to be associated with the cooperative arrangement on the 1D ridges. The formation of the cooperative arrangement with *mono*-modal distribution provides a path to realize uniform dots as well as the control of the spatial arrangement.

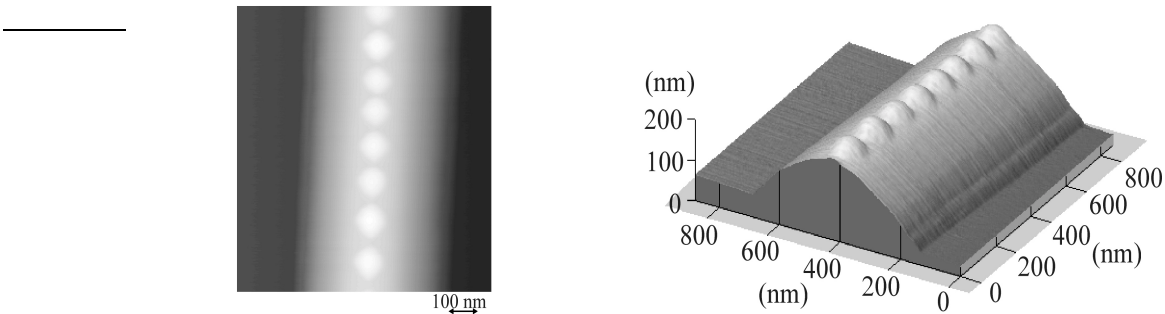


Fig. 2 (a) 2D and (b) 3D AFM images of self-assembled Ge dots on $\langle 110 \rangle$ -oriented Si stripe mesa with a base width of $0.55 \mu\text{m}$. One-dimensional cooperative arrangement of Ge dots is formed on the ridge of the Si mesa after the deposition of 10 ML Ge at a growth temperature of 600°C .

(b) Characterization

Figure 3 shows two typical bright-field cross-sectional TEM images of the as-grown sample and the

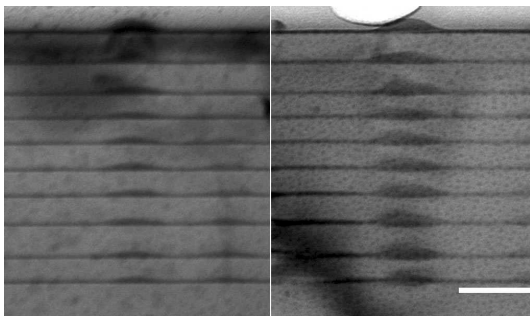


Fig. 3 Cross section TEM image taken from the sample with ten layers of Ge quantum dots, showing the vertical alignment. (b) a) as-grown, b) annealed at 900°C for 5 min. TEM images showed that the dots were dislocation-free.

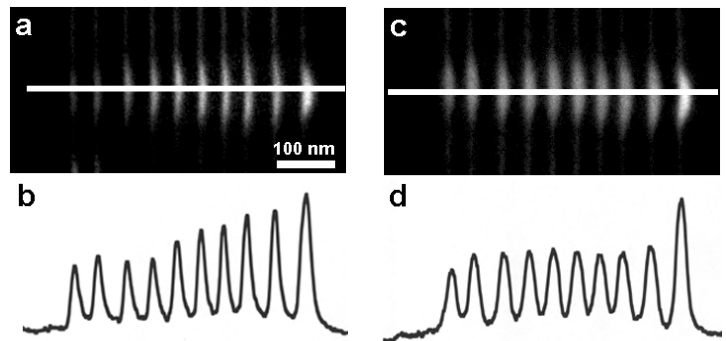


Fig. 4. (a) A Ge elemental map of the as-grown sample; (b) the intensity profile taken from the white line passing through the center of the island column in (a); (c) a Ge elemental map of the annealed sample; (d) the intensity profile taken from the white line passing through the center of the island column in (c).

sample annealed at 900°C for 5 min. As shown in the images, the GeSi dots were still present after annealing. Figure 4(a) is a typical energy filtered image (EFI) of the as-grown sample showing Ge map. From the image it is clear that the island size increases continuously in upper layers. Figure 4(b) is the intensity profile along the

white line passing through the center of the island column in Fig.4(a). The intensity also increases continuously in upper layers which means continuous increase of Ge concentration in upper layer islands. Figure 4(c) is a typical EFI of the annealed sample showing Ge map. An interesting annealing effect is shown in Fig. 4(d), the intensity profile obtained along the white line passing through the island column center in Fig. 4(c). The intensity profile suggests the equalization of average Ge concentration among buried islands in different layers.

Fig. 5 presents the photoluminescence spectrum taken from a sample with 10-layer Ge dots at the temperature of 4.5 K, showing the contribution from Ge wetting layers and Ge quantum dots. In addition to the PL peaks from Si, there are two separate components, which come from the islands and the wetting layer,

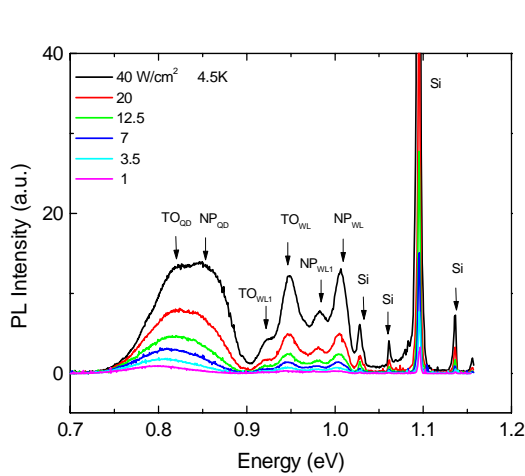


Fig. 5. PL spectra of the 10 layer Ge/Si (001) islands under different excitation power levels measured at 4.5K. The peaks at about 0.8 eV

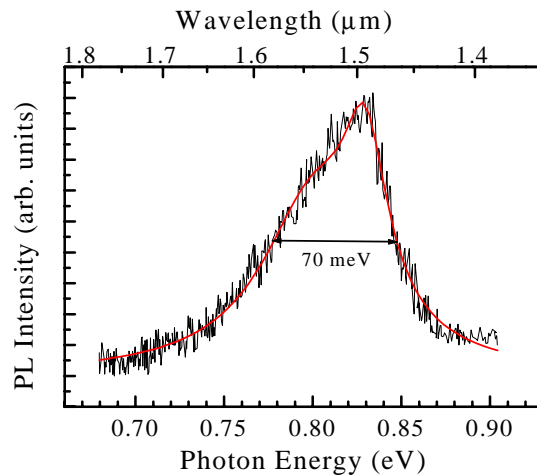


Fig. 6 Photoluminescence spectrum taken at room temperature, only showing the peaks at about 0.8 eV or 1.55 μm attributed to Ge quantum dots. The full width at half maximum of the double peak is about 70 meV

respectively. The TO and NP PL lines originating from the first wetting layer and the upper wetting layer are indicated by TO_{WL1} , NP_{WL1} , TO_{WL} , NP_{WL} , respectively. The PL band from the islands could be deconvoluted into two gaussian line-shaped peaks which are indicated by TO_{ID} and NP_{ID} , respectively.

The photoluminescence from Ge dots at about 0.8 eV was observed at room temperature as shown in Fig. 6, albeit peaks from Ge wetting layers and Si disappeared. This is due to the quantum confinement effect, therefore, the excitons in dots quench at higher temperature at about 100 K compared with 25 K for Ge wetting layers. The merit of photoluminescence from Ge dots at room temperature will perhaps impact the optoelectronic applications.

(c) Controlled positioning of Ge dots

Further studies on the control of Ge dot positioning have been conducted and the AFM results are shown in Figs. 7 and 8. Four pyramidal Ge dots are located at the corners of the pre-grown Si mesas as shown in Fig. 7. Several different configurations of the positioning have also been observed with the variation of the Ge thickness deposited. One dot on each Si mesa has been obtained at the growth temperature of 700°C shown in Fig. 8. Given the results of the vertical strain-induced ordering and the success of forming localized quantum dots by a homoepitaxial template, the possibility is that the strain distribution present in a 3-D feature such as a strained layer SiGe SEG be used to further control and to allow for more precise placement of quantum dot arrays.

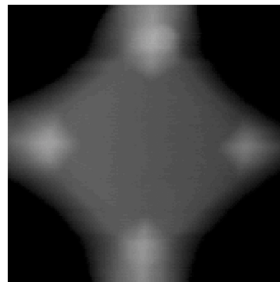
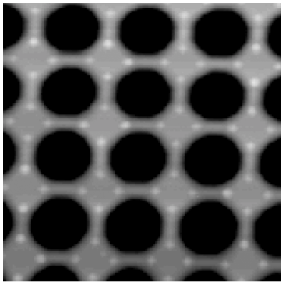


Fig. 7 Two-dimensional AFM images of 2D arrangement of Ge dots with 0.8 nm Ge at growth temperature of 600°C, (left) Four Ge dots are arranged on each unit of Si mesas; (right) Magnified view of a unit cell in (a).

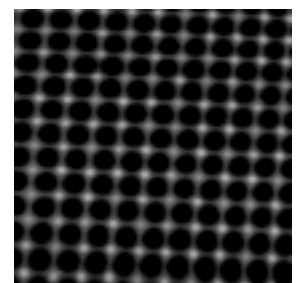
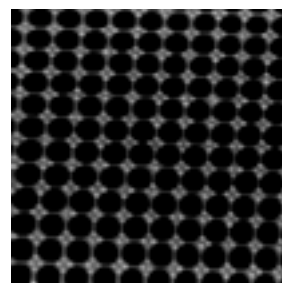


Fig. 8 Two-dimensional AFM images of 2D arrangement of Ge dots. (left) Growth temperature is 650°C, four Ge dots are arranged on each unit of Si mesas; (right) Growth temperature is 700°C, only one Ge dot is arranged on each unit of Si mesas.

II: Mid-IR absorption of Ge quantum dots

(a) Intersubband absorption in boron-doped Ge quantum dot superlattices

A 200 nm undoped Si buffer layer is grown first, followed by 20 periods of thin heavily boron-doped Ge quantum dot layers sandwiched with two 6 nm undoped Si films. In this work, the samples (JL039, JL088 and JL038) with different Ge layer thicknesses are prepared to study the size dependence of the subband energy. Similar samples with single-layered Ge quantum dots grown on the surface are examined with AFM showing typical base dimensions of 420, 450 Å, and heights of 40, 45, for samples JL039, and JL088 respectively. Sample JL038 has no dots but wetting layers only. The nonuniformity of the dot size is estimated to be $\pm 10\%$. The area density of the dots for samples JL039, and JL088 are $1 \times 10^8 \text{ cm}^{-2}$ and $2 \times 10^8 \text{ cm}^{-2}$, respectively.

Figure 9 shows the measured absorption spectra of the samples JL039, JL088 and JL038 at the 0° polarization angle (i.e., electric field having a component in the growth direction as described in the following). For sample JL039, absorption peaks are found at near 2000 cm^{-1} (5 μm) and 1350 cm^{-1} (7.4 μm), which are

attributed to intersubband transitions in the Ge quantum dots and the Ge wetting layer, respectively. The full widths at half maximum (FWHM) of the absorption peak at 5 μm for the sample JL039 is about 100 meV, and is considerably larger than the intersubband peak width observed in InGaAs/GaAs quantum dot superlattice (~ 13 meV). The size nonuniformity of quantum dots is a possible factor. Another reason is that the nonparabolicity of the hole bands can play a strong role in the broadening of the absorption peaks as was observed in the quantum well case. Similar to sample JL039, absorption peaks are found at 1650 cm^{-1} ($6\ \mu\text{m}$) and 1350 cm^{-1} ($7.4\ \mu\text{m}$) for sample JL088, which are again due to transitions in the Ge quantum dots and the Ge wetting layer, respectively. For sample JL038, however, only one absorption peak near $7.4\ \mu\text{m}$ is found, which is believed to be due to the absorption in the Ge wetting layer.

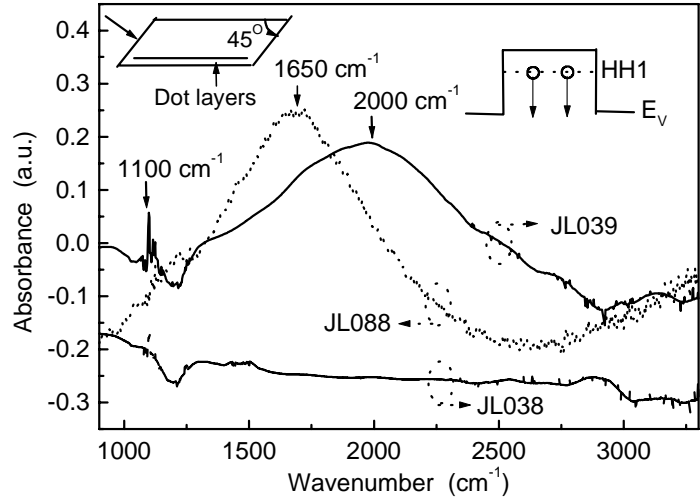


Fig.9 FTIR absorption spectra for samples JL039, JL088 and JL038 taken at room temperature. Background spectra have been subtracted. The top left inset is the waveguide structure used in the experiments. The top right inset shows the possible mechanism of the transition.

The almost same absorption peak position in three Ge wetting layers for the three samples is due to the fact that the thicknesses of wetting layers (usually 3–6 Å) of the samples are about the same under the almost same growth conditions (for example, growth temperature). From Fig. 9, all of three samples have peaks near 1100 cm^{-1} and 1450 cm^{-1} , which are mainly due to the strong infrared absorption by SiO_2 and water bands in the spectral range of interest.

The observed intersubband transitions in the Ge dots can be compared with the calculated subband energies. Here, we assume a Ge dot is a simple infinite-barrier box, and do not consider exciton-like effects as well as depolarization effects. Thus, the allowed energies in the dot can be evaluated precisely as follows:

$$E_{n,k,l} = \frac{\pi^2 \hbar^2}{2m^*} \left(\frac{n^2}{L_x^2} + \frac{k^2}{L_y^2} + \frac{l^2}{L_z^2} \right), \quad n, k, l = 1, 2, 3, \dots \quad (1)$$

where m^* is Ge hole effective mass. The effective masses used for calculation are $0.30m_0$ and $0.044m_0$ for the heavy and light holes, respectively. L_x and L_y are base dimensions while L_z is the height of the dots. For sample JL039, the first two terms of the equation are omitted because L_x and L_y (42 nm) are much larger than L_z (4 nm). The calculated results show that there are two heavy hole bound states at 78 and 311 meV. The light hole bound states exist near the top of the Si barrier potential or higher due to the small effective mass and small dot size, and thus are not occupied. The energy separation between the first two heavy hole states is 233 meV, which is close to the measured peak energy of 247 meV ($5\ \mu\text{m}$ peak). Similar calculation has been done for

sample JL088 and the calculated energy separation of 184 meV is also close to the measured peak energy of 205 meV (6 μm peak). It seems easy for us to conclude that the observed absorption peaks of 5 μm and 6 μm are due to the transitions between the first two heavy hole bound states. Nevertheless, the absorption could also arise from an intraband transition between the dot ground states to the continuum states since the line shape was asymmetric, characteristic of a bound-to-continuum transition. This has been schematically shown in the inset of the Fig. 9. In addition, other effects such as valence band mixing, depolarization, and exciton-like shifts may also contribute the observed peak energies.

(b) Intersubband absorption in modulation-doped Ge quantum dot superlattice

The sample (JL104) consists of a 200-nm undoped Si buffer layer, 30 periods of Ge quantum dots sandwiched between two 6-nm boron-doped Si layers, and a 50-nm undoped Si cap layer. The doping density in the Si layers is as high as $5 \times 10^{18} \text{ cm}^{-3}$. The size of the dots is obtained from a single-layered sample with an identical growth condition to be 2-3 nm in height and 20-30 nm in base diameter.

Fig.10 shows the measured absorption spectrum with unpolarized infrared light. An absorption peak is found at 1880 cm^{-1} , which is believed to come from the inter-sub-level transition of holes in the Ge quantum dots. The inset of the Fig.10 shows a possible transition, i.e., bound-to-continuum transition which is responsible for the observed absorption. The FWHM of 62 meV is considerably larger than the inter-sub-level peak width observed in the InGaAs/GaAs quantum dot superlattice ($\sim 13 \text{ meV}$). Obviously, the size nonuniformity of quantum dots may be a contributing factor.

Additionally, the nonparabolicity of the hole bands may play a strong role in the broadening of the absorption peaks as was observed in the quantum well case. Background absorption mainly associated with the free carriers is observed as a monotonously increasing absorption towards low energy.

III: Photodetectors based on Ge quantum dots

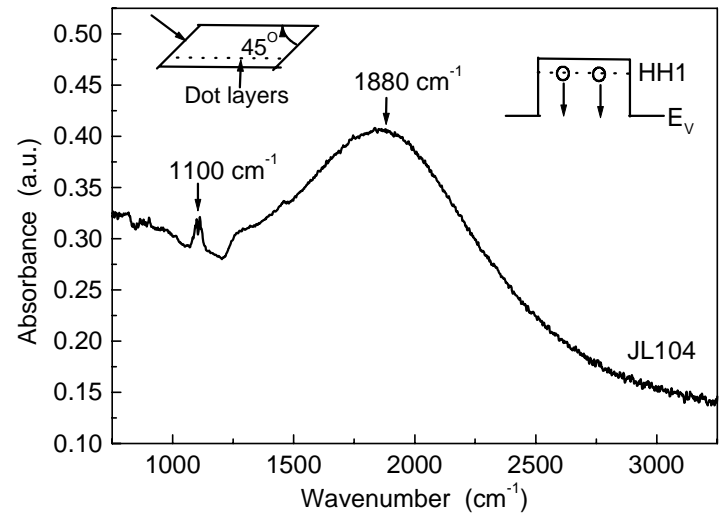


Fig.10 FTIR absorption spectrum of the modulation-doped sample JL104. No polarization of the incident infrared light is employed. An absorption peak at 1880 cm^{-1} is due to the inter-sub-level absorption in the Ge quantum dots.

For photoresponse characterization, p-i-n photovoltaic diodes were designed and fabricated. Ten layers of Ge dots separated by Si as the active region were sandwiched by p⁺ and n⁺ Si layers. The total nominal deposition thickness of Ge is about 20 nm. Deposition was performed at 550 °C, and the growth speed is 0.1 nm/sec. Mesa was defined by dry etching with CF₄/O₂. The mesa size is 150x300 μm². A 220 nm SiO₂ isolation layer was deposited by PECVD at 300 °C. Al/Ti layer was deposited with Sloan e-beam evaporation to form the contact. Then the wafer was cut into dices and packaged to T0-5 holders to make the back contact. The top contact was finished by a HYBOND wirebonding equipment. A schematic drawing of the device structure is shown in Figure 11 (a). Shown in Fig. 11 b is the plane view image of the diode. It is clear that spectacular morphology is kept after the processing.

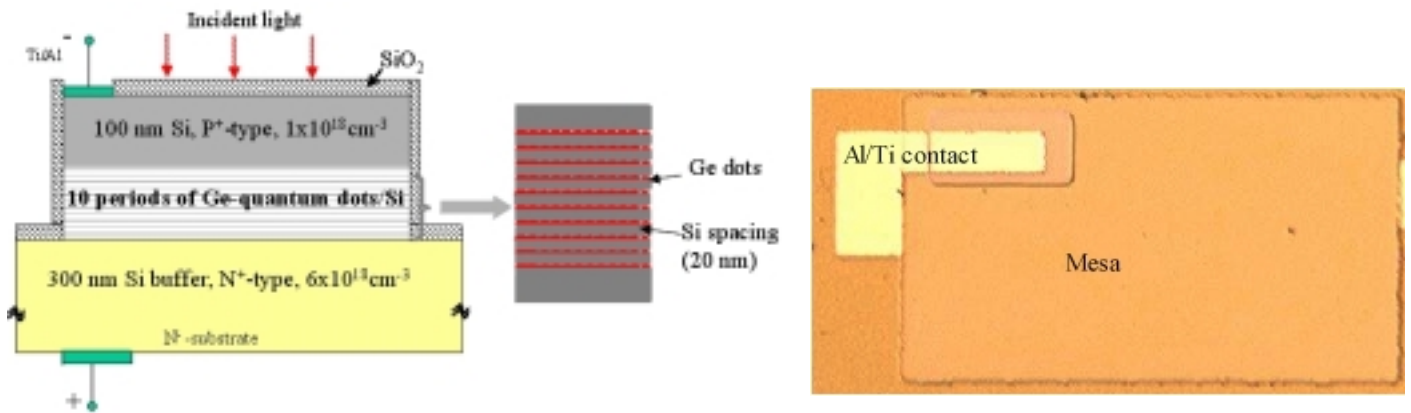


Figure 11. (a) Schematic drawing of the cross section view of the device structure.
 (b) plane view of the processed sample. It shows that spectacular morphology is kept.

I-V measurement was performed with HP41420A at room temperature. A typical plot is shown in Figure 12. The result shows good rectifying characteristics of the current. Low dark current, $3 \times 10^{-5} \text{ A/cm}^2$ at -1 V was

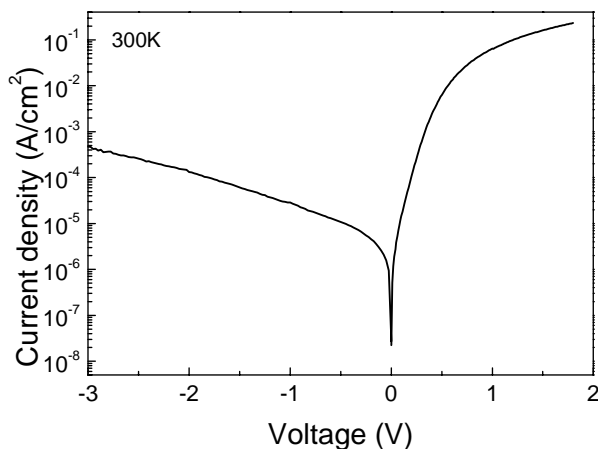


Figure 12, I-V characteristics of the p-i-n diodes at room temperature. It shows a dark current of $3 \times 10^{-5} \text{ A/cm}^2$ at -1 V.

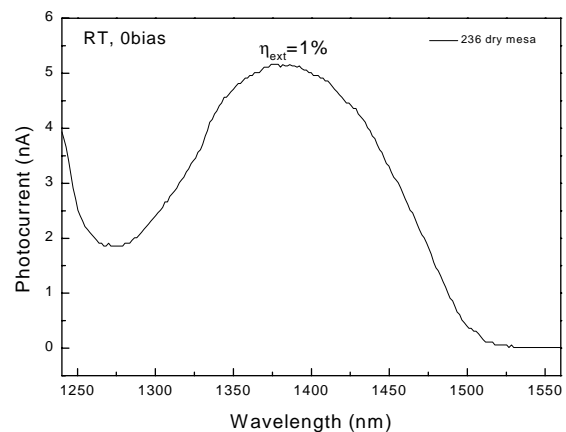


Figure 13. A typical photocurrent spectrum of the p-i-n diode at room temperature with zero bias. An external quantum efficiency of 1% was obtained.

obtained. The breakdown voltage is around 5V.

For the photoresponse measurement, a tungsten lamp was used as the light source. The light passes through a 34-cm monochromator and casts normally onto the diodes. The measurement was performed at room temperature. Figure 13 shows a typical response spectrum at zero bias. It shows that the diodes have strong response at 1.3-1.5 μm . The increase below 1.25 μm is due to the absorption of Si. The redshift of this cutoff edge comparing to pure Si ($\sim 1.1 \mu\text{m}$) is due to the intermixing between Si and Ge or the strain effect. Calibrated by a Newport optical power meter, an external efficiency of 1% at 0 bias is observed at 1.4 μm .

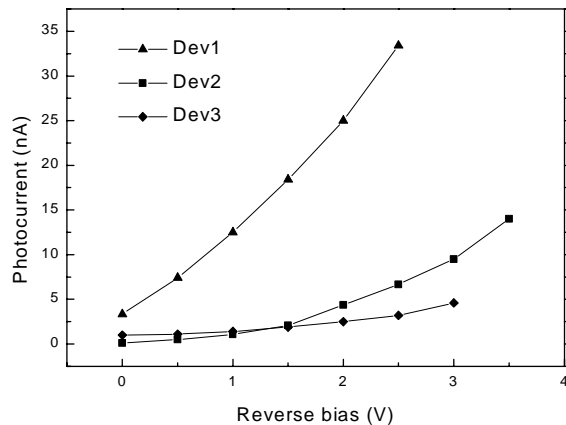


Figure 14. Photocurrent of three devices at different biases. The excitation power is 300 nW. The maximum efficiency ever reached is 8%.

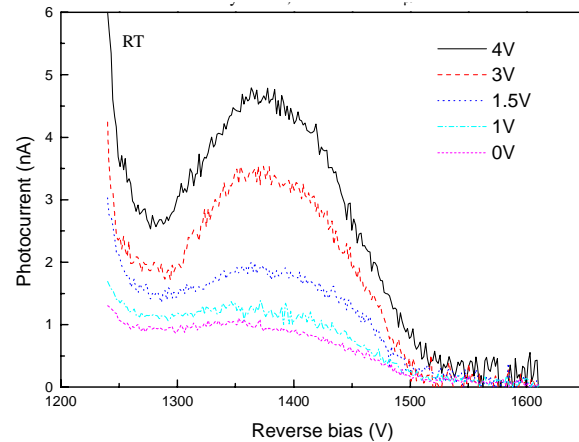


Figure 15. Response spectra at different biases.

The photoresponse intensity increases while applying a reverse bias. This effect is shown in figure 14. Three devices were measured at the range of 0-4V. The response wavelength was selected at 1.4 μm . The different behavior among devices is maybe due to the gravity of the surface recombination, especially along the sidewall of the mesa. The maximum external efficiency ever reached is 8% at 2.5 V. The calculated absorption of the nominal Ge thickness of 20 nm is less than 0.5%. This indicates that a great enhancement of the absorption was realized. The enhancement of the absorption is probably due to the scattering of the light by dots in the active layer, and this increases the chance of the photons being absorbed by the dots. The highest efficiency that reported from Si/Ge strained layer superlattice grown by MBE is 12% at 1.3 μm , by H. Presting, with waveguide coupling mode. The detector length is 4 mm. By further improving the device fabrication to reduce the dark current, it is believed that higher voltage can be applied and hence higher quantum efficiency can be reached. In figure 15, the spectra at different bias are shown. No obvious change of the shape and shift of the absorption edge was detected in the studied range. But it is possible that at higher bias, e.g., near breakdown voltage, the edge at long wavelength may shift to longer, even to 1.55 μm .

(6) Listing of all publications.

- [1]. *Controlled arrangement of self-organized Ge islands on patterned Si (001) substrates*. Jin, G.; Liu, J.L.; Thomas, S.G.; Luo, Y.H.; Wang, K.L.; Nguyen, B.-Y.. Applied Physics Letters, **75**, (1999), p.2752-4
- [2]. *Cooperative arrangement of self-assembled Ge dots on pre-grown Si mesas*, Jin G, Liu JL, Luo YH, Wang KL, THIN SOLID FILMS 380: (2000), p.169-172
- [3]. *Control of the arrangement of self-organized Ge dots on patterned Si(001) substrates*, Jin G, Liu JL, Luo YH, Wang KL, THIN SOLID FILMS 369: (2000), p49-54
- [4]. *Temperature-dependent morphology of three-dimensional InAs islands grown on silicon*, P. C. Sharma, K. W. Alt, D. Y. Yeh, and K. L. Wang, Appl. Phys. Lett., **75**, (1999) p. 1273-1275
- [5]. *Formation of nanometer-scale InAs islands on silicon*, Sharma PC, Alt KW, Yeh DY, Wang D, Wang KL, Journal of Electrical Materials, **28**, (1999), p. 432-436
- [6]. *Intersubband absorption in boron-doped multiple Ge quantum dot*, J.L.Liu, W.G. Wu, A. Balandin, G.L. Jin, K.L. Wang, Applied Physics Letters, **74**, 185 (1999).
- [7]. *Raman scattering from a self-organized Ge dot superlattice*, J.L.Liu, Y.S.Tang, and K.L.Wang, T.Radetic and R. Gronsky, Applied Physics Letters, **74**, 1863 (1999).
- [8]. *Growth and optical properties of self-organized Ge quantum wires on Si (111) substrates*, G. Jin, Y. S. Tang, J. L. Liu, and K. L. Wang, Applied Physics Letters, **74**, 2471 (1999).
- [9]. *Observation of inter-sub-level transitions in modulation-doped Ge quantum dot*. Liu, J.L.; Wu, W.G.; Balandin, A.; Jin, G.; Luo, Y.H.; Thomas, S.G.; Lu, Y.; Wang, K.L. Applied Physics Letters, **75**, AIP, 20 (1999), p.1745-7.
- [10]. *Infrared spectroscopy of intraband transitions in Ge/Si quantum dot superlattices*, Wen-Gang Wu; Jian-Lin Liu; Yin-Sheng Tang; Wang, K.L. Superlatt. Microstruct., **26**, (1999), p.219-27.
- [11]. *Influence of misfit strain on {311} facet development in selective epitaxial growth of Si/sub 1-x/Ge/sub x/Si(100) grown by gas-source molecular beam epitaxy*, U'Ren, G.D.; Goorsky, M.S.; Wang, K.L. Thin Solid Films, **365**, (no.1), (2000), p.147-50.
- [12]. *Optical and acoustic phonon modes in self-organized Ge quantum dot superlattices* Liu, J.L.; Jin, G.; Tang, Y.S.; Luo, Y.H.; Wang, K.L.; Yu, D.P.. Applied Physics Letters, **76**, (2000), p.586-8.
- [13]. *Study of phonons in self-organized multiple Ge quantum dot*, J.L. Liu, G. Jin, Y.S. Tang, Y.H. Luo, Y. Lu, K.L. Wang, D.P. Yu, J. Electr. Mat., **29**, (2000), p.554-6.
- [14]. *Perfect alignment of self-organized Ge islands on pre-grown Si stripe mesa*, G. Jin, J.L. Liu, S.G. Thomas, Y.H. Luo, K.L. Wang, Nguyen, B.Y., Applied Physics A **70**, (2000), p.551-4.
- [15]. *Regimented placement of self-assembled Ge dots on selectively grown Si mesas*, G. Jin, J. L. Liu, and K. L. Wang, Applied Physics Letters, **76**, (2000), p.3591-3.

- [16] “*High-quality strain-relaxed SiGe films grown with low temperature Si buffer.*” Luo, Y.H.; Wan, J.; Forrest, R.L.; Liu, J.L.; Goorsky, M.S.; Wang, K.L. *Journal of Applied Physics*, vol.89, (no.12), AIP, 15 June 2001. p.8279-83.
- [17] “*Compliant effect of low-temperature Si buffer for SiGe growth.*” Luo, Y.H.; Wan, J.; Forrest, R.L.; Liu, J.L.; Jin, G.; Goorsky, M.S.; Wang, K.L. *Applied Physics Letters*, vol.78, (no.4), AIP, 22 Jan. 2001. p.454-6.
- [18] “*Optical study of SiGe films grown on low-temperature Si buffer,*” Y.H. Luo, J. Wan, J. L. Liu, K. L. Wang, 2001 MRS Spring Meeting, San Francisco, April 16-20, 2001
- [19] “*High quality SiGe films grown by low temperature Si buffer,*” Y.H. Luo, J. Wan, J.L. Liu, G. Jin, K.L. Wang, SRC Techcon-2000, Sept. 21-24 (2000), Phoenix, AZ. Minneapolis, MN, *Bulletin of the American Physical Society*, Vol. 45, No. 1, page 801 (S36 140)
- [20] “*Normal-incidence Ge quantum-dot photodetectors at 1.5 μm based on Si substrate,*” S. Tong, J. L. Liu, J. Wan, and Kang L. Wang, *Applied Physics Letters*, 80, 1189 (2002)

(7) List of all participating scientific personnel showing any advanced degrees earned by them while employed on the project

G. L. Jin	graduated student, Ph.D. awarded
J. L. Liu	graduated student
J. Wan	postdoctoral researcher
S. Tong	postdoctoral researcher

(8) Report of Inventions: N/A

(9) Bibliography

(10) Appendixes